Academic Journal of Science and Technology,
JUN, 2024, vol.3, No.1, p171-180

Computational Study of Photodegradation Mechanism of Alminoprofen, The Basis for Designing New NSAIDs

Klefah A. K. Musa*

1. Department of Medicinal Chemistry, Pharmacy College, El-Mergib University, Al-Khoms, Libya

ABSTRACT

Alminoprofen (AP) is 2-(4-((2-methlyallyl)amino)phenyl)propanoic acid, or 2-[4-(2-methylprop-2-enylamino)phenyl]propanoic acid. It has a role as a lipoxygenase, a phospholipase A2 and a cyclooxygenase 2 inhibitor. Due to these enzyme's inhibitions, it is used as anti-inflammatory, anti-rheumatic and anti-pyretic agent in treatment of inflammatory and rheumatic disorders. Because of the AP is belonging to the propionic aromatic acid structure derivatives and is very similar to the ibuprofen molecule and due to the photosensitivity adverse effects related to this group, the present work focuses upon the photosensitivity photodegradation mechanism of AP. This has been done using the HF-DFT/TD-DFT framework by applying the hybrid functional B3LYP level of theory. Similar to other NSAIDs studied previously, the obtained results of AP from the computed energies and properties of various species show that the deprotonated form dominates at physiological pH, is the susceptible species for photodegradation more than the neural form. In addition, the former species will not be able to decarboxylate from a singlet excited states with high efficiency. In contrast, after it undergoes intersystem crossing, the excited triplet state of the deprotonated form will decarboxylate, with very high efficiency. Molecular orbitals, energies of various species, various energy barriers, reactive radical species, the reactions of radical species with macromolecules and more throughout alminoprofen photodegradation mechanism have been discussed in more details in this work.

KEYWORDS: *alminoprofen, NSAID, decarboxylation, photodegradation, DFT, TD-DFT.*

* *Corresponding author:* klefah.musa@gmail.com

INTRODUCTION

Alminoprofen (AP) belongs to non-steroidal anti-inflammatory drugs (NSAIDs), its chemical structure is quite similar to ibuprofen. The isobutyl group in ibuprofen is replaced by a (2-methylprop-2-en-1-yl)amino group. It is nothing except a substituted aniline, so the chemical name of AP is 2-(4-((2-methlyallyl)amino)phenyl)propanoic acid, or 2-[4-(2-methylprop-2-enylamino)phenyl]propanoic acid (Figure 1). It has a role as a lipoxygenase, a phospholipase A2 and a cyclooxygenase 2 inhibitor. Due to these enzyme's inhibitions, it is used as anti-inflammatory, anti-rheumatic and anti-pyretic agent in treatment of inflammatory and rheumatic disorders [1]. The phospholipase A2 enzyme targeted by AP is likely the secretory phospholipase A2. The mechanism of action of AP was investigated in an invitro study where the effect of AP on phospholipase A2 and cyclooxygenase of the cells in culture is examined. In addition, an in vivo study of AP in which the inflammatory action of both exogenous and endogenous phospholipase A2 is also investigated in the rats. Both studies suggest the anti-inflammatory action of AP is dual inhibiting the activity of both phospholipase A2 and cyclooxygenase 2 (COX-2) enzymes [2, 3].

The previous studies show that the AP in clinical treatment of inflammatory diseases as COX-2 inhibitor is expressed more efficacy than that of ibuprofen. In addition, the pharmacological profile and mode of analgesic action of AP are apparently different from other acidic NSAIDs. The anti-inflammatory and analgesic activity produced by AP are more potent than that of ibuprofen [4]. In contrast to other NSAIDs such as ibuprofen, the AP is considered as a new type of nonsteroidal anti-inflammatory agent [5]. The AP shows a relatively potent anti-pyretic activity where it does not involve an inhibition of cyclooxygenase at a central site that considered as an antipyretic mechanism of NSAIDs, instead the AP mechanism of action is competitive with leukocytic pyrogen at a site in the central nerves system [6]. In addition, the AP is very useful for pediatric and adults' patients in the treatment of post exodontic pain [7]. The AP exerts a combined inhibition of prostaglandin E2 synthesis, leukocyte chemotaxis and lysosomal enzyme release so, it has a potent anti-inflammatory and analgesic activity in sodium urate crystal-induced inflammations [8].

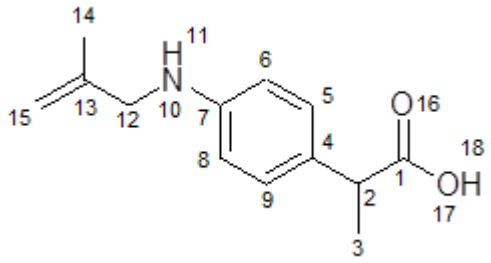

Figure 1. chemical structure of AP; numbering is used throughout the study

Generally, Nonselective NSAIDs have various side effects such as gastrointestinal side effects (e.g., peptic ulcer, dyspepsia, and bleeding), renal adverse effects (e.g., renal vasoconstriction leading to acute renal failure and worsening of underlying hypertension, as well as electrolytes and fluid abnormalities, in addition to renal cell cancer risk may be increased), cardiovascular effects, central nervous system adverse effects (e.g., psychosis, aseptic meningitis and cognitive dysfunction), anaphylaxis, other allergic and pseudoallergic reactions as well as skin reactions [9]. NSAIDs are from the most drugs causing photosensitivity due to they are reported on more frequently than others and they are designed to inhibit inflammation in fact cause light-initiated inflammation. Phenylpropionic acid derivatives group is the most NSAIDs causing photosensitivity. The NSAIDs causing cutaneous photosensitivity appears to be elicited by a phototoxicity mechanism [10]. Moreover, NSAIDs with the propionic aromatic acid structure derivatives such naproxen can induce skin photosensitivity and DNA photocleavage as well as photo-hemolytic activity in red blood cells [11-13]. Interestingly, from other side, in animal studies naproxen shows that it reduces the tumor multiplicity and decrease the number of cutaneous tumor lesions [11, 14, 15].

Because of the AP is belonging to the propionic aromatic acid structure derivatives and is very similar to the ibuprofen molecule and due to the photosensitivity adverse effects related to this group mentioned above, we, in the current work, focus upon the AP photo-degradation mechanism. It is clarified in the Figure 2, and discussed below in details. In which, we have investigate the possible photoinduced decarboxylation process of AP and the followed reactions those cause the formation of reactive oxygen species (ROS), and considered as the main reactions initiators in lipid peroxidation processes.

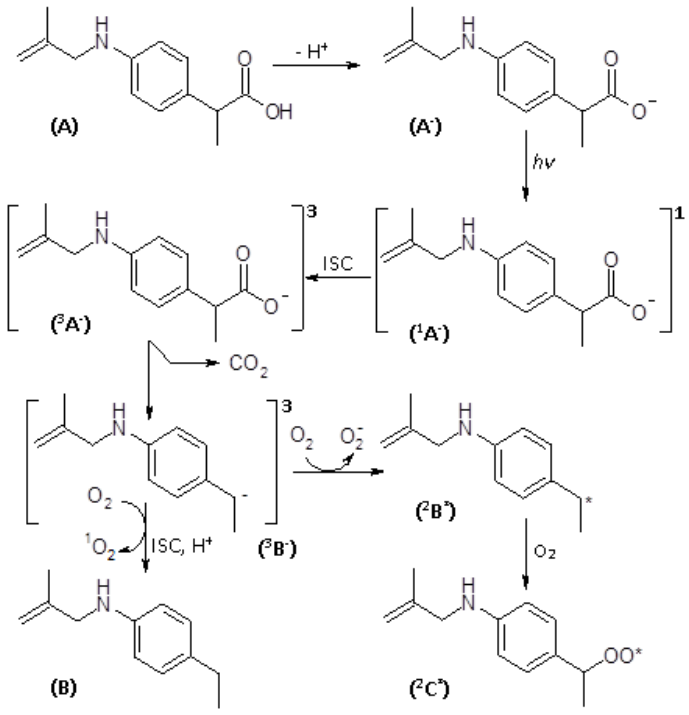

Figure 2. Schematic photodegradation mechanism of AP.

COMPUTATIONAL METHODOLOGY

The hybrid functional B3LYP as one form of HF-DFT frameworks is used [16-18], together with middle size basis set 6-31G(d,p). It was used in order to obtain the optimized structures of all molecules described in Figure 2 using the GAUSSIAN 03 package [19]. The basis set used herein in the current work is taken depending upon our pervious study for a similar molecular size drug diclofenac and its main photoproduct (8-chlorocarbazole) in there we have done test calculations using a range of basis sets (e.g., 6-31g(d,p) and 6-311g(d,p) with or without diffuse functions) [20]. The results obtained from this test show that the effects on absorption spectra and transitions are within only a few nanometers, and therefore, for computational reasons we have had used the B3LYP-6-31G(d,p) level of theory throughout the AP photodegradation mechanism herein. At the obtained optimized geometries of all species under the study, zero-point vibrational energies (ZPE) were evaluated, as were free energy corrections at T = 298 K. Single-point calculations were performed at the same level of theory using the integral equation formalism of the polarized continuum model (IEF-PCM) of Tomasi and co-worker that is in order to describe the effect of the surrounding medium [21-23]. Bulk water was included as solvent with a value of 78.9 for the dielectric constant ε.

Excitation energies, electron and proton affinities and ionization potentials were obtained at the same level of theory. Using Mulliken population analysis, spin densities as well as atomic charges were extracted.

Time dependent DFT (TD-DFT) [24-26] calculations were performed for excitation energies and when exploring the possibility for the decarboxylation process to occur from different excited states of AP. The excitation energies tend to be overestimated by approximately 0.2 eV at this level of theory, leading to a slight blue-shift of the peaks in the computed spectra. Furthermore, solvent effects have very little influence on the absorptions, under the methodology employed herein, and were hence not included in the TD-DFT calculations. The atomic numbering scheme used for the various molecules (Figure 2) follows that of Figure 1.

RESULTS AND DISCUSSION

REDOX CHEMISTRY OF AP:

The redox properties of the alminoprofen parent compound A are investigated herein. In Figure 3, we have displayed the optimized structures of AP (A), its radical anion and radical cation (A*- and A*+), and its deprotonated species (A-). The main difference in these optimized structures is in the C1-C2 bond length change, which is the decarboxylated responsible bond, from 1.522 Å in the neutral parent compound to 1.594 Å in the corresponding deprotonated species. Very little change in this bond length was noted between the radical anion and radical cation compared to the parent neutral structure. From the obtained calculated energies shown in the Table 1, the electron affinity (EA) and ionization potential (IP) in gas phase accounted as -25.5 and 155.6 Kcal/mol, respectively. The negative EA of the anionic form implies that it is unstable in this case. Once we applying the bulk solvation via the IEFPCM method, the EA and IP are accounted instead to be 12.2 and 112.1 Kcal/mol, respectively, this is in a line with our previous studies with very similar molecule ibuprofen [27].

The computed absolute and relative ZPE-corrected energies in gas phase, free energies and the dipole moments obtained in aqueous solution are displayed in the Table 1. We noted that among the various species studied herein the anionic form (A*-) is the most stable species in the aqueous solution. Solvent stabilization of this species is computed to be 37.7 Kcal/mol, this is similar to the obtained results of ibuprofen and ketoprofen in our previous studies as accounted 40.6 Kcal/mol and 45 Kcal/mol, respectively [27, 28]. The IP from other side is accounted about 155.6 Kcal/mol in gas phase which is reduced under the stabilization effect of the aqueous solution where the Gibbs free energy of the cation form is 112 Kcal/mol. The free energy difference between the protonated parent compound (A) and its deprotonated species (A-) is computed to be 353 Kcal/mol, which is reduced to 296.3 Kcal/mol in aqueous solution. This is again in a line with previous results obtained for similar NSAIDs the ibuprofen, ketoprofen and flurbiprofen compounds [27-29].

The local charge on the carboxylic moiety (O16-C1-O17-(H18)) of the protonated parent compound of AP (A) and its radical anion (A*-), radical cation (A*+) and deprotonated acid species (A-) are obtained from the Mulliken atomic charge distributions of the various species that displayed in the Table 2, are -0.056, -0.289, 0.033, and -0.706 e-, respectively. These findings are in a line with the computed dipole moment of these species in Table 1. The difference in computed dipole between the parent neutral compound and its deprotonated counterpart is more than 19 D, because of the highly localized negative charge. The Mulliken atomic charges of the decarboxylated species are mainly localized on C3, C14 of methyl moieties and N10 which connected to the aromatic system of the AP (see Table 2).

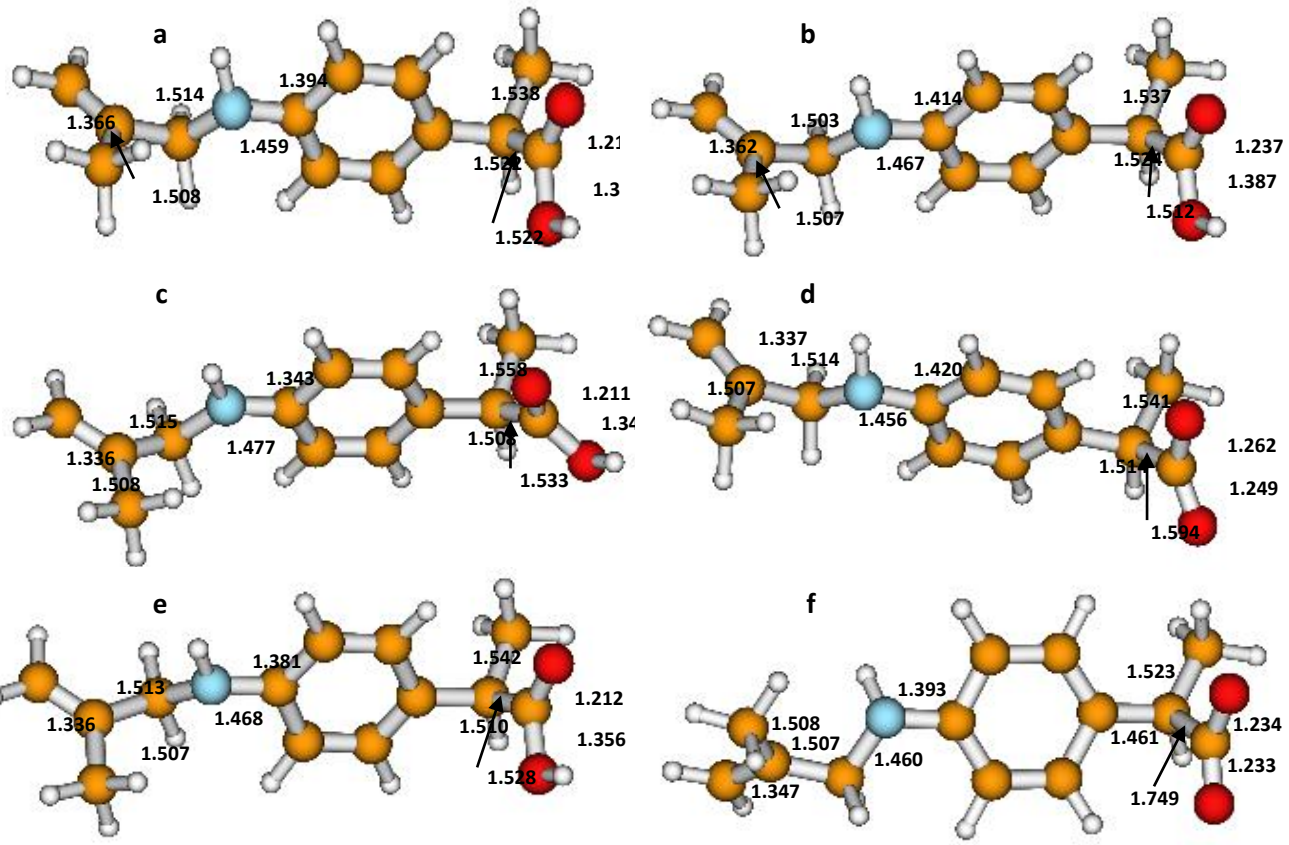

Figure 3. Optimized structures of AP, (a) the neutral (protonated) ground state; **A**, (b) the radical anion; $\mathbf{A}^{-*}$, (c) the radical cation; $\mathbf{A}^{+*}$, (d), the deprotonated ground state; $\mathbf{A}^{-}$, (e) the neutral triplet state species; $^{3}\mathbf{A}$, and (f) the deprotonated triplet state species; $^{3}\mathbf{A}^{-}$.

Table 1 B3LYP/6-31G(d,p) ZPE-corrected electronic energies in gas phase, and IEFPCM- B3LYP/6-31G(d,p) Gibbs free energies in aqueous solution. The absolute energies in a.u., relative energies in kcal/mol, and the dipole moments in (debye) in aqueous solution.**:**

System	$E_{(ZPE)}$	$\Delta E_{(ZPE)}$	ΔG_{aq}^{298}	$\Delta\Delta G_{aq}^{298}$	μ_{aq}
A (singlet)	-710.570162	0	-710.637339	0	3.05
$\mathbf{A}^{-*}$ (doublet)	-710.529571	25.47	-710.656815	-12.22	9.16
$\mathbf{A}^{+*}$ (doublet)	-710.322246	155.57	-710.458721	112.08	5.26
$^{3}\mathbf{A}$ (triplet)	-710.450382	75.16	-710.522410	72.12	4.83
$\mathbf{A}^{-}$ (singlet)	-710.007474	353.09	-710.165095	296.34	22.45
$^{3}\mathbf{A}^{-}$ (triplet)	-709.903076	418.60	-710.047783	369.95	19.84
$^{3}\mathbf{B}^{-*}$ (triplet)	-521.333095	0	-521.449504	0	5.10
$^{1}\mathbf{B}^{-*}$ (singlet)	-521.387285	-34.00	-521.507973	-36.69	10.56
B (singlet)	-522.015746	-428.37	-522.067186	-387.60	1.48
$\mathbf{B}^{*}$ (doublet)	-521.383498	-31.63	-521.437103	7.78	2.38
$^{2}\mathbf{C}^{*}$ (doublet)	-671.728308	***	-671.789934	***	5.88

In the Table 3, we list the unpaired electron densities of AP species those illustrated in Figure 2. The spin densities of the radical anion localized on the phenyl ring mainly on C9 and on the methylene moiety C15 and account as 0.209 and 0.171 e, respectively. Instead, for the radical cation the spin densities localized mainly on the atoms of the aromatic system and on the nitrogen atom (N10), on the latter it accounts 0.384 e. The spin densities of the unpaired electrons of either the protonated or the deprotonated form in the triplet state are localized all over the phenyl ring and with a small extent, in the neutral triplet state, to the nitrogen atom N10 of the AP molecule. For the decarboxylated species (3B- and 2B*) the main portion of the spin densities localized to the C2 atom (connected to the carboxylic moiety in the parent AP compound) and accounts as 0.696 and 0.735 e, respectively. For the oxygenated doublet species (2C*) the spin density is localized mainly on the (–OO*) group as seen in Table 3.

In order to shed more light on the AP photochemistry, we in Figure 4 show the computed highest occupied and lowest unoccupied molecular orbitals (HOMOs and LUMOs) of the protonated and deprotonated AP forms. We noted that the HOMO, HOMO-1 and HOMO-2 of the neutral species are mainly localized on the phenyl ring with lesser extent on the nitrogen atom (N10), totally localized on the aromatic system, and on isobutenylamino moiety, respectively. The LUMO and LUMO+1 of the protonated form are both mainly localized on the aromatic systems with lesser extent to the propionic acid moieties. Instead, the LUMO+2 of the same species is localized on the peripheral isobutenylamino moiety. In contrast to the neutral form the deprotonated species of AP show a different orbital pattern. In which the three HOMOs are all localized on the carboxylic moieties of the propionic acid. The LUMO of the deprotonated form is localized on the isobutenylamino moiety of the AP. Lastly, the LUMO+1 and LUMO+2 of the deprotonated species are localized on the phenyl rings and for the second with lesser extent to the nitrogen atom (N10). The MOs pattern difference between the two species of AP (protonated and deprotonated) is manifested in the Mulliken atomic charge distribution on the carboxylic moiety, that in the first form is only -0.056 e-, instead, in the second it is -0.706 e-. This difference in the MO distributions of the neutral versus deprotonated of AP plays an important role in their photochemical behaviors.

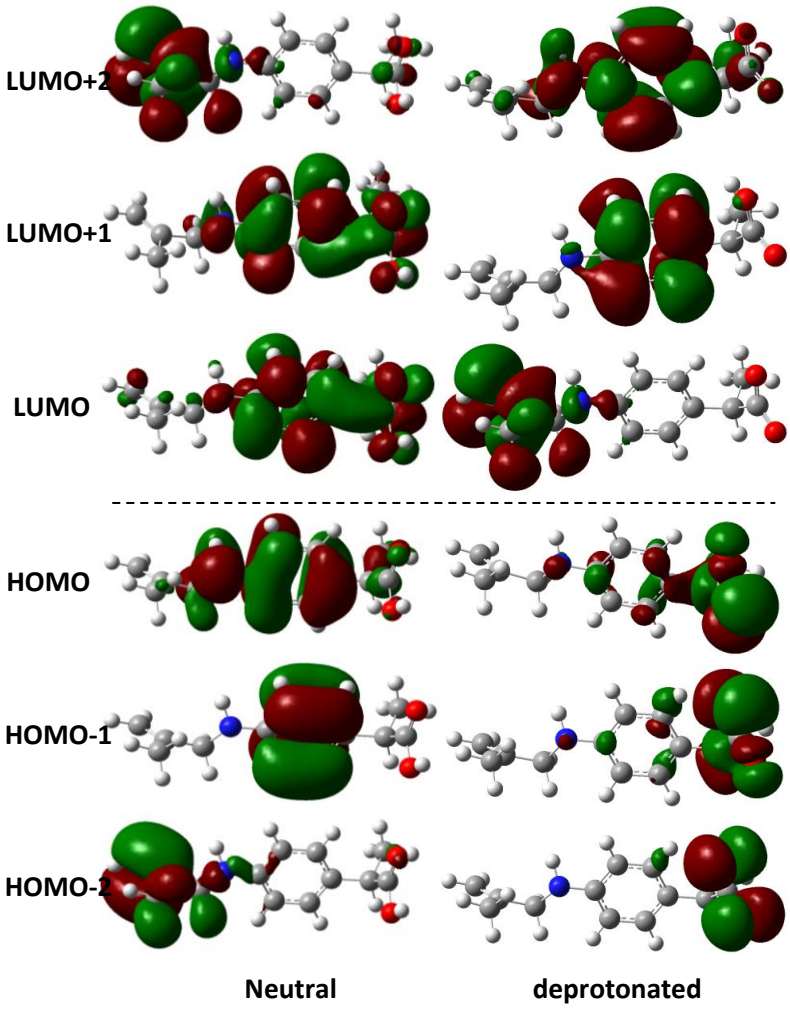

Figure 4. Molecular orbitals of AP: Neutral form (the left) and deprotonated anion (the right).

Table 2. Mulliken atomic charges (B3LYP/6-31G(d,p) level) for selected atoms in AP and its photoproducts Figure 2. For atomic labelling see Figure 1.

System	C1	C3	C7	C14	C15	N10	H11	O16	O17	H18
A (singlet)	0.590	-0.298	0.326	-0.356	-0.279	-0.601	0.250	-0.474	-0.490	0.318
A-* (doublet)	0.520	-0.289	0.267	-0.346	-0.331	-0.590	0.210	-0.561	-0.531	0.283
A+* (doublet)	0.595	-0.318	0.360	-0.365	-0.254	-0.513	0.311	-0.447	-0.461	0.346
3A (triplet)	0.588	-0.298	0.262	-0.360	-0.282	-0.540	0.261	-0.469	-0.491	0.318
A- (singlet)	0.537	-0.294	0.290	-0.353	-0.289	-0.597	0.235	-0.621	-0.622	
3A- (triplet)	0.566	-0.305	0.288	-0.350	-0.307	-0.575	0.219	-0.533	-0.542	
3B- (triplet)		-0.331	0.316	-0.343	-0.350	-0.586	0.204			
B- (singlet)		-0.310	0.130	-0.354	-0.298	-0.577	0.210			
B (singlet)		-0.304	0.318	-0.356	-0.280	-0.590	0.249			
B* (doublet)		-0.352	0.315	-0.357	-0.279	-0.597	0.251			
2C* (doublet)		-0.318	0.332	-0.357	-0.278	-0.601	0.253			

Table S2. Atomic spin densities (B3LYP/6-31G(d,p) level) on selected atoms for the radical species of AP and its photoproducts. For atomic labeling see Figure 1.

System	C2	C4	C5	C6	C7	C8	C9	C15	N10
A-* (doublet)				0.108	0.121		0.209	0.171	
A+* (doublet)		0.369	0.107	0.193		0.194			0.384
3A (triplet)		0.547	0.526	0.148	0.438	0.636	0.239		0.226
3A- (triplet)		0.264		0.469	0.303	0.147	0.582		
3B-* (triplet)	0.696		0.309	0.172	0.157		0.427	0.256	
B* (doublet)	0.735	0.193	0.217	0.110	0.211	0.118	0.230		
2C* (doublet)	O inner = 0.306 and O outer = 0.688								

EXCITATION OF ALMINOPROFEN AND ITS DEPROTONATED SPECIES:

The excitation of A in its neutral or deprotonated form of AP to the first excited singlet state S1 (or a higher lying singlet states Sn) which in turn followed by radiationless decay to S1 is the initial step in the photodegradation of AP, again followed by intersystem crossing (ISC) to the first excited triplet state as seen in the photodegradation scheme (Figure 2). Because of the pKa value of the deprotonated acid (accounts 4.86±0.50 "Predicted" [30], 5.02 "Exp" [31]); due to the pKa is low the AP will predominantly in its deprotonated (acidic) form clear difference. Each species (protonated/deprotonated) of AP show two main absorption peaks with distinguish wavelengths and oscillator strengths. The two absorption peaks of the neutral form are in the 200-280 nm range (the first peak lies at 220 nm, whereas, the second one located at 252 nm of the spectrum; with almost equal oscillator strengths (f) around 0.181 and 0.191, respectively, the second peak with a weak shoulder extension ended around 320 nm. In contrast, for the second absorption peak of the deprotonated species lies to a higher wavelength compared to the first form and it extends to 340 nm of the spectrum. The UV spectrum between 200 and 400 nm of the deprotonated form displays two clear peaks at around 220 and 320 nm with oscillator strengths (f) 0.272 and 0.087, respectively, with a relative intensity ratio of 3:1. From experimental point of view, the UV spectrum of AP shows that there is a main peak at 255 nm with a small shoulder at 290 to 320 nm [32]. This is in a perfect agreement with the present results for the protonated (neutral) species, the present methodology applied herein, we should take into our considerations that there is the blue-shifts of the absorptions by approximately 10–15 nm in the current wavelength regime. at physiological pH (7.4), and the structural features changes upon the deprotonation discussed above, thus in turn the photodegradation of AP is more likely to occurs from A- species. Relating to the orbitals of the neutral and the deprotonated as clarified in Figure 4, the computed UV spectra of these species are markedly different as seen in the Figure 5.

Furthermore, similar to the difference in the orbitals pattern between the neutral (protonated) and deprotonated species of AP, the computed UV spectra of these species also show clear difference. Each species (protonated/deprotonated) of AP show two main absorption peaks with distinguish wavelengths and oscillator strengths. The two absorption peaks of the neutral form are in the 200-280 nm range (the first peak lies at 220 nm, whereas, the second one located at 252 nm of the spectrum; with almost equal oscillator strengths (f) around 0.181 and 0.191, respectively, the second peak with a weak shoulder extension ended around 320 nm. In contrast, for the second absorption peak of the deprotonated species lies to a higher wavelength compared to the first form and it extends to 340 nm of the spectrum. The UV spectrum between 200 and 400 nm of the deprotonated form displays two clear peaks at around 220 and 320 nm with oscillator strengths (f) 0.272 and 0.087, respectively, with a relative intensity ratio of 3:1. From experimental point of view, the UV spectrum of AP shows that there is a main peak at 255 nm with a small shoulder at 290 to 320 nm [32]. This is in a perfect agreement with the present results for the protonated (neutral) species, the present methodology applied herein, we should take into our considerations that there is the blue-shifts of the absorptions by approximately 10–15 nm in the current wavelength regime.

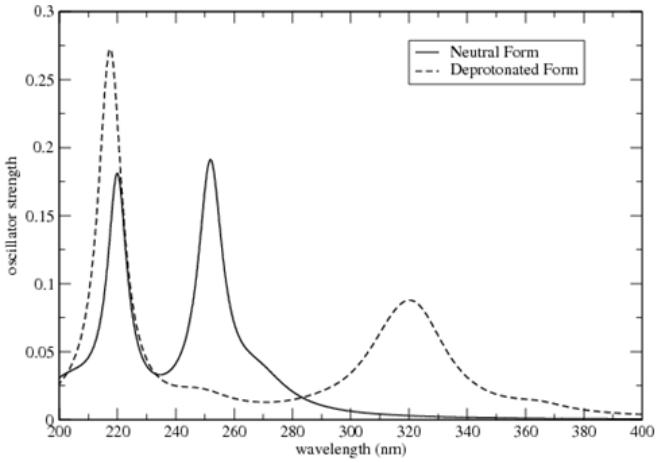

Figure 5. Computed absorption spectra in the 200-400 nm range of the protonated (solid) and deprotonated (dashed) forms of AP, obtained at the TD-B3LYP/6-31G(d,p) level.

Once the neutral (A) and the deprotonated (A-) forms of AP are excited the corresponding first excited singlet state will be formed, then upon the ISC lead to formation of corresponding triplet state. The optimized triplet state of the protonated form (3A) lies 75.16 Kcal/mol above the optimized ground state (A), whereas for the deprotonated form which most likely is the responsible for photodegradation process (as discussed above), the corresponding free energy difference between (3A-) and (A-) is 65.51 Kcal/mol. Under the inclusion of the bulk solvation, these computed values are very little affected. This is in very agreement with the results obtained with other NSAIDs [27-29, 33-35].

In the Figure 3, we show the optimized molecules of the protonated and the deprotonated triplet states of AP, For the former, there is very small changes in geometry of optimized triplet state compared with the parent molecule are noted, instead, for the second one, there is an elongation in the C1-C2 bond length from 1.594 Å in the optimized singlet ground state of the deprotonated form to 1.749 Å in the triplet state of this species. This bond is responsible for the photo-decarboxylation process as seen in Figure 2. In order to investigate the energy barrier required for decarboxylation process from the triplet state of the deprotonated species. The responsible bond (C1-C2 bond) was scanned outwards from the optimized value (1.794 Å) in step of 0.1 Å. In each new point, the molecules were re-optimized, and calculate the energies. The resulting energy curve is shown in the Figure 6. The obtained energy barrier for decarboxylation to take place from the first excited

triplet state of the AP deprotonated species is only of 0.63 Kcal/mol, at the C1-C2 distance of the transition state is approximately 2.049 Å. This is again with a line of the obtained results of the similar NSAIDs previously studied [e.g., 27, 33].

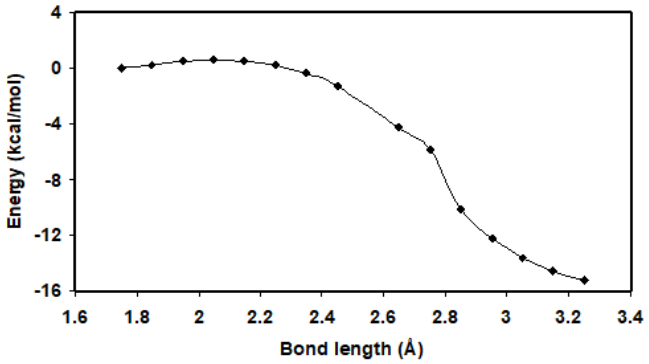

Figure 6. The energy barrier for decarboxylation from the first excited triplet state of the deprotonated species of AP

THE FATE OF DECARBOXYLATED ALMINOPROFEN:

The deprotonated species of AP as described above is responsible for the decarboxylation especially from its triplet state with a very low barrier around 0.63 Kcal/mol. The various pathways upon the decarboxylation as depicted in the scheme photodegradation mechanism (Figure 2) can be summarized in the following reactions.

Once the AP molecule is deprotonated and excited into the triplet state, there are various pathways of this species to ended with different species according to the proposed photodegradation mechanism illustrated above. In first reaction (a), the AP deprotonated excited to triplet species decarboxylates with very low energy barrier (approximately, 0.63 Kcal/mol, Figure 6) forming decarboxylated (3B-) species, the energy difference between triplet state species (3B-) and the ground singlet sate (1B-) is 34 Kcal/mol in vaccum, which under the bulk solvation effect computed to be 36.69 Kcal/mol. Which in turn, under intersystem crossing (ISC) and proton addition, utilizing oxygen molecules and forming the reactive singlet oxygen species and the ground state of decarboxylated (B) species. The second reaction (b): In which, the redaical doublet species (2B*) the computed energy for this step accounted to be 31.63 Kcal/mol, this energy obatianed in vaccum and under the effect of bulk solvation is changed dramaticaly to be 7.78 Kcal/mol. Formation of oxygen anion species is also expected during this pathway. The third reaction in photodegradation mechanism is reaction (c) which is no thing except formation of peroxide derivative of (2C*) by the reaction between the redaical doublet species (2B*) and a molecule of oxygen. This process was explored via scanning the responsible bond distance (C2-OO) in step of 0.1 Å. We in Figure 7 display the energy diagram of this addition. The computed energy differenc between the product of the proxyl radical (2C*) and the starting point with the reactants (2B*) and molecular oxygen, which separated by 3.3 Å, is 19.5 Kcal/mol. Figure 7 show that this reaction is strictly exothermic with a obvious change in slope at C-O distance of about 2.1 Å. Interestingly, under aerobic conditions, this reaction is exergonic and will proceed spontaneously without an energy barrier. These findings are similar with that of obtained for other NSAIDs previously studied at the same level of theory [27-29, 33-35]. These above pathways could be summarized according to the following equations from (1) to (3).

$$^3A^- \xrightarrow{-CO_2} {}^3B^- \xrightarrow[O_2]{ISC,\ H^+} B + O_2 \qquad (1)$$

$$^3A^- \xrightarrow{-CO_2} {}^3B^- \xrightarrow{O_2} {}^2B^* + O_2^- \qquad (2)$$

$$^2B^* \xrightarrow{O_2} {}^2C^* \qquad (3)$$

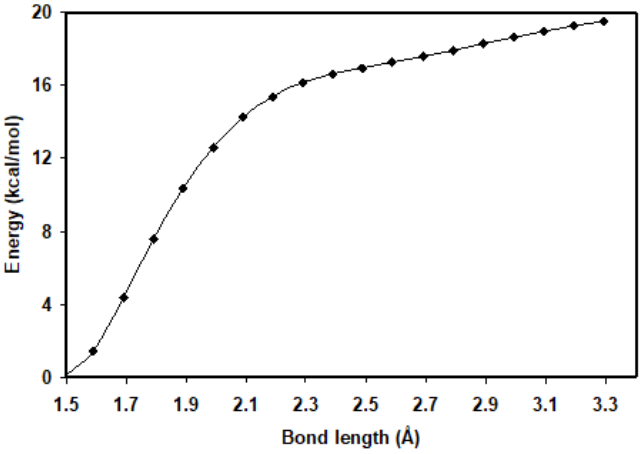

Figure 7. Formation of the peroxyl radical 2C* species by addition reaction between 2B* and molecular oxygen

The reactive oxygen species formed throughout the AP photodegradation mechanism, according to the above equations will be terminated, regarding to the following pathways (reactions i-iii). In addition to pervious reactions (1-3), formation of peroxyl radical species (2C* = 2BOO*) according to reaction (i) is considered as a good initiator of lipid peroxidation reactions. Moreover, the removal of a hydrogen atom from a lipid molecule according to reaction (ii) will lead to the formation of a lipid radical species (L*). The latter species which in turn reacts with molecular oxygen yielding a lipid peroxyl radical (LOO*) according to reaction (iii).

$$^2B^* + O_2 \longrightarrow {}^2BOO^* \text{ (i.e., } {}^2C^*) \qquad \textbf{(i)}$$

$$^2BOO^* + LH \longrightarrow B(OOH) + L^* \qquad \textbf{(ii)}$$

$$L^* + O_2 \longrightarrow LOO^* \qquad \textbf{(iii)}$$

In addition, the radical species produced throughout these reactions have capability to react with other macromolecules systems such as proteins and DNA. These processes are creating what is known as the propagation of radical damage cascade system. This propagation system will begin and continue until terminated by, for example, the antioxidants action such as with vitamin E or by the radical-radical addition.

CONCLUSION

Alminoprofen (AP) belongs to NSAIDs. Chemically, it is quite similar to ibuprofen. Since, isobutyl group in ibuprofen is replaced by a (2-methylprop-2-en-1-yl)amino group. It is nothing except a substituted aniline, so the chemical name of AP is 2-[4-(2-methylprop-2-enylamino)phenyl]propanoic acid. The anti-inflammatory action of AP is dual inhibiting the activity of both phospholipase A2 and cyclooxygenase 2 (COX-2) enzymes Because of the AP is very similar to the ibuprofen molecule and due to the photosensitivity adverse effects related to this group mentioned above, we, in the current work, focus upon the photosensitivity photodegradation mechanism of AP, using the HF-DFT/TD-DFT framework in the form of the hybrid functional B3LYP level of theory.

The obtained results show that the HOMO, HOMO-1 and HOMO-2 of the neutral species are mainly localized on the phenyl ring with lesser extent on the nitrogen atom (N10), totally localized on the aromatic system, and on isobutenylamino moiety, respectively. In contrast to the neutral form the deprotonated species of AP show a different orbitals pattern, since HOMOs are all localized on the carboxylic moieties of the propionic acid. This is in a line with the obtained Mulliken charge distribution.

The computed AP absorption show that the two absorption peaks of the neutral form are in the 200-280 nm range (the first peak lies at 220 nm, whereas, the second one located at 252 nm of the spectrum; with almost equal oscillator strengths. Whereas, the deprotonated form displays two clear peaks at around 220 and 320 nm with oscillator strengths (f) 0.272 and 0.087, respectively. The main process in the AP photodegradation mechanism is the decarboxylation from the predominant species under physiological pH (the deprotonated form) of AP. The obtained the energy barrier for decarboxylation is mainly from the triplet state of the deprotonated species which accounted only 0.63 Kcal/mol, at the C1-C2 distance of the transition state is approximately 2.049 Å, this is with same line with other NSAIDs studied previously. There are several pathways of photodegradation after decarboxylation process ended with various reactive radical oxygen species, producing with reaction of macromolecules what is known as the propagation of radical damage cascade system. This propagation system will begin and continue until terminated by, for example, the antioxidants action and/or the radical-radical addition.

REFERENCES

1. National Center for Biotechnology Information (2022). PubChem Compound Summary for CID 2097, Alminoprofen. https://pubchem.ncbi.nlm.nih.gov/compound/Alminoprofen.
2. Raguenes-Nicol C, Russo-Marie F, Domage G, Diab N, Solito E, Dray F, Mace JL, Streichenberger G. Anti-inflammatory mechanism of alminoprofen: action on the phospholipid metabolism pathway. Biochem. Pharmacol. 1999, 57(4):433-43. doi: 10.1016/s0006-2952(98)00312-8.
3. Fujiyoshi T, Iida H and Hayashi I. Pharmacological profile and mode of action of alminoprofen, a nonsteroidal anti-inflammatory drug. Jap. Pharmacol. Ther. 1990,18: 159–180.
4. Fujiyoshi T, Iida H, Kuwashima M, Dozen M, Taniguchi N, Ikeda K. Pharmacological Profile of Alminoprofen among Four Writhing Models of Mice Caused by Kaolin, Zymosan, Acetylcholine and Phenylquinone. Journal of Pharmacobio-Dynamics, 1990, 13(1):44-48.
5. Kojima E, Tamura N, Higashide Y, et al. Effects of alminoprofen on the allergic reactions. Nihon Yakurigaku zasshi. Folia Pharmacologica Japonica. 1990, 96(6):315-321. DOI: 10.1254/fpj.96.6_315.
6. Maeda E, Uematsu T. The anti-pyretic mechanism of alminoprofen. Nihon Yakurigaku Zasshi. 1991, 98(6):457-66. Japanese. doi: 10.1254/fpj.98.6_457.
7. Sugahara T, Sakuda M, Yoshida H, Michi KI, kurachi Y, Kanemoto K, Nagumo M. Clinical evaluation of alminoprofen (Minalfen®) on postexodontic pain. Oral Therapeutics and Pharmacology. 1992, 11(3):147-59.
8. Maeda E, Hujiyoshi T, Uematsu T. Effects of alminoprofen on sodium urate crystal-induced inflammation. Nihon Yakurigaku zasshi. Folia Pharmacologica Japonica. 1991, 98, (6):467-474. DOI: 10.1254/fpj.98.6_467.
9. Solomon, Daniel H. Nonselective NSAIDs: Overview of adverse effects. UpToDate [internet]. UpToDate Inc.[updated 03.03 2020, cited 03.03 2021] Available from: https://www. uptodate.com (2020).
10. Kochevar IE. Phototoxicity of Nonsteroidal Inflammatory Drugs: Coincidence or Specific Mechanism? Arch Dermatol. 1989, 125, (6):824–826. doi:10.1001/archderm.1989.01670180096016.
11. George EA, Baranwal N, Kang JH, Qureshi AA, Drucker AM, Cho E. Photosensitizing Medications and Skin Cancer: A Comprehensive Review. Cancers (Basel). 2021, 12;13(10):2344. doi: 10.3390/cancers13102344.
12. Costanzo L.L., De Guidi G., Condorelli G., Cambria A., Famà M. Molecular mechanism of naproxen photosensitization in red blood cells. J. Photochem. Photobiol. B. 1989, 3:223–235. doi: 10.1016/1011-1344(89)80064-8.
13. De Guidi G., Giuffrida S., Condorelli G., Costanzo L.L., Miano P., Sortino S. Molecular mechanism of drug photosensitization. IX. Effect of inorganic ions on DNA cleavage photosensitized by naproxen. Photochem. Photobiol. 1996, 63:455–462. doi: 10.1111/j.1751-1097.1996.tb03069.x.
14. Mikulec C.D., Rundhaug J.E., Simper M.S., Lubet R.A., Fischer S.M. The chemopreventive efficacies of nonsteroidal anti-inflammatory drugs: The relationship of short-term biomarkers to long-term skin tumor outcome. Cancer Prev. Res. 2013, 6:675–685. doi: 10.1158/1940-6207.CAPR-13-0064.
15. Gonzalez Maglio D.H., Paz M.L., Ferrari A., Weill F.S., Nieto J., Leoni J. Alterations in skin immune response throughout chronic UVB irradiation-skin

cancer development and prevention by naproxen. Photochem. Photobiol. 2010, 86:146–152. doi: 10.1111/j.1751-1097.2009.00623.x.
16. Becke, A. D., Density-functional thermochemistry .3. the role of exact exchange. Journal of Chemical Physics 1993, 98, (7):5648-5652.
17. Stephens, P. J.; Devlin, F. J.; Chabalowski, C. F.; Frisch, M. J., AB-initio calculation of vibrational absorption and circular-dichroism spectra using density-functional force-fields. Journal of Physical Chemistry 1994, 98, (45):11623-11627.
18. Lee, C. T.; Yang, W. T.; Parr, R. G., Development of the colle-salvetti correlation-energy formula into a functional of the electron-density. Physical Review B 1988, 37, (2):785-789.
19. MJT Frisch, G. W. S., H. B.; Scuseria, G. E.; Robb, M. A.; Cheeseman, J. R.; Montgomery, J. A., Jr.; Vreven, T.; Kudin, K. N.; Burant, J. C.; Millam, J. M.; Iyengar, S. S.; Tomasi, J.; Barone, V.; Mennucci, B.; Cossi, M.; Scalmani, G.; Rega, N.; Petersson, G. A.; Nakatsuji, H.; Hada, M.; Ehara, M.; Toyota, K.; Fukuda, R.; Hasegawa, J.; Ishida, M.; Nakajima, T.; Honda, Y.; Kitao, O.; Nakai, H.; Klene, M.; Li, X.; Knox, J. E.; Hratchian, H. P.; Cross, J. B.; Bakken, V.; Adamo, C.; Jaramillo, J.; Gomperts, R.; Stratmann, R. E.; Yazyev, O.; Austin, A. J.; Cammi, R.; Pomelli, C.; Ochterski, J. W.; Ayala, P. Y.; Morokuma, K.; Voth, G. A.; Salvador, P.; Dannenberg, J. J.; Zakrzewski, V. G.; Dapprich, S.; Daniels, A. D.; Strain, M. C.; Farkas, O.; Malick, D. K.; Rabuck, A. D.; Raghavachari, K.; Foresman, J. B.; Ortiz, J. V.; Cui, Q.; Baboul, A. G.; Clifford, S.; Cioslowski, J.; Stefanov, B. B.; Liu, G.; Liashenko, A.; Piskorz, P.; Komaromi, I.; Martin, R. L.; Fox, D. J.; Keith, T.; Al-Laham, M. A.; Peng, C. Y.; Nanayakkara, A.; Challacombe, M.; Gill, P. M. W.; Johnson, B.; Chen, W.; Wong, M. W.; Gonzalez, C.; Pople, J. A. , Gaussian 03, rev. B.02; Gaussian, Inc.: Wallingford, CT, . 2004.
20. Musa, K. A. K.; Eriksson, L. A., Photodegradation mechanism of the common non-steroid anti-inflammatory drug diclofenac and its carbazole photoproduct. Physical Chemistry Chemical Physics 2009, 11, (22):4601-4610.
21. Mennucci, B.; Tomasi, J., Continuum solvation models: A new approach to the problem of solute's charge distribution and cavity boundaries. Journal of Chemical Physics 1997, 106, (12):5151-5158.
22. Cossi, M.; Scalmani, G.; Rega, N.; Barone, V., New developments in the polarizable continuum model for quantum mechanical and classical calculations on molecules in solution. Journal of Chemical Physics 2002, 117, (1):43-54.
23. Cances, E.; Mennucci, B.; Tomasi, J., A new integral equation formalism for the polarizable continuum model: Theoretical background and applications to isotropic and anisotropic dielectrics. Journal of Chemical Physics 1997, 107, (8): 3032-3041.
24. Bauernschmitt, R.; Ahlrichs, R., Treatment of electronic excitations within the adiabatic approximation of time dependent density functional theory. Chemical Physics Letters 1996, 256, (4-5):454-464.
25. Casida, M. E.; Jamorski, C.; Casida, K. C.; Salahub, D. R., Molecular excitation energies to high-lying bound states from time-dependent density-functional response theory: Characterization and correction of the time-dependent local density approximation ionization threshold. Journal of Chemical Physics 1998, 108, (11):4439-4449.
26. Stratmann, R. E.; Scuseria, G. E.; Frisch, M. J., An efficient implementation of time-dependent density-functional theory for the calculation of excitation energies of large molecules. Journal of Chemical Physics 1998, 109, (19):8218-8224.
27. Musa, Klefah AK, and Leif A. Eriksson. "Theoretical study of ibuprofen phototoxicity." The Journal of Physical Chemistry B. 2007, 111, (46):13345-13352.
28. Musa, Klefah AK, Jon M. Matxain, and Leif A. Eriksson. "Mechanism of photoinduced decomposition of ketoprofen." Journal of medicinal chemistry. 2007, 50, (8):1735-1743.
29. Musa, Klefah AK, and Leif A. Eriksson. "Photochemical and photophysical properties, and photodegradation mechanism, of the non-steroid anti-inflammatory drug Flurbiprofen." Journal of Photochemistry and Photobiology A: Chemistry. 2009, 202, (1):48-56.
30. https://amp.chemicalbook.com/ProductChemicalPropertiesCB7885929_EN.htm
31. Andrew G. Mercader, Mohammad Goodarzi, Pablo R. Duchowicz, Francisco M. Fernandez, Eduardo A. Castro, Predictive qspr study of the dissociation constants of diverse pharmaceutical compounds. Chem Biol Drug Des, 2010, 76:433–440. doi: 10.1111/j.1747-0285.2010.01033.x
32. https://jpdb.nihs.go.jp/kyokuhou/files/000152738.pdf
33. Klefah A. K. Musa and Leif A. Eriksson. Theoretical study of the phototoxicity of naproxen and the active form of nabumetone. The Journal of Physical Chemistry A. 2008, 112, (43):10921-10930. DOI: 10.1021/jp805614y.
34- Klefah A. K. Musa and Leif A. Eriksson. Photodegradation mechanism of nonsteroidal anti-inflammatory drugs containing thiophene moieties: Suprofen and tiaprofenic acid. The Journal of Physical Chemistry B. 2009, 113, (32):11306-11313. DOI: 10.1021/jp904171p.
35. Klefah A. K. Musa and Leif A. Eriksson Computational Studies of the Photodegradation Mechanism of the Highly Phototoxic Agent Benoxaprofen. ACS Omega. 2022, 7, (33):29475-29482. DOI: 10.1021/acsomega.2c03118